

SIZING AN EXCLUSION REGION AROUND LUNAR-SURFACE PROTECTED SITES FOR DISPOSAL VIA IMPACT

J. Gangestad

The Aerospace Corporation, 14745 Lee Road, Chantilly, Virginia, USA, Email: joseph.gangestad@aero.org

ABSTRACT

This paper reports on an analysis to determine an appropriate exclusion region around protected sites when planning lunar impact as an end-of-life disposal option. Impact with the lunar surface has been a favored disposal option since the beginning of the space age, but until recently only a small number of national scientific agencies operated spacecraft at the Moon. Today, interest in the Moon is reaching a fever pitch, with dozens of missions in development or announced, including government and commercial actors around the world. Many of these operators already have used or will use impact as a disposal option, but national and international rules that govern end-of-life disposal provide few specifics on how an impact should be designed to preserve the safety of other actors at the Moon and the lunar environment overall. Following a review of the literature on impact ejecta, lunar regolith, and historical impact examples, we develop expressions that model the mass density of ejecta as a function of range from the spacecraft impact site and the kinetic energy of ejecta particles when they impact the surface at range. We identify from the literature threshold kinetic energies that correspond to damage or injury of protected assets. For each threshold kinetic energy, we use the modeled areal mass density of ejecta to estimate the probability of damage or injury for a protected asset as a function of range. To account for scenario-dependent parameters of the impactor (i.e., its mass, density, and impact velocity), we vary those parameters in a Monte Carlo fashion based on historical examples and record the extremal ejecta range for a given kinetic-energy threshold and probability of damage. This approach gives us a near-worst case for the range that an ejecta particle could reach for that energy and probability of damage. We consider kinetic energies of 3 to 150 J, probability of damage from 10^{-5} to 10^{-3} , and two empirical lunar-surface models that bound the properties of lunar regolith. To select an overall limiting impact range, we apply risk thresholds comparable to those accepted for LEO and geocentric applications. We find that a range of approximately 20 km is adequate to achieve this risk equivalence under our conservative assumptions.

Keywords: debris; disposal; cislunar; moon; impact.

1. INTRODUCTION

In the United States, both government and commercial space missions must comply with debris-mitigation and disposal rules. Government missions comply with the Orbital Debris Mitigation Standard Practices (ODMSP) [35], and U.S. government organizations derive formal requirements from the ODMSP and document them in instructions or standards that space missions in their organization must comply with (see, for example, [26] and [31]). Commercial spacecraft in the United States comply with disposal rules promulgated by the Federal Communications Commission (FCC), which oversees commercial communications licenses. The FCC's disposal rules are largely consistent with the ODMSP, albeit with some differences. For example, the ODMSP specify a maximum 25-year lifetime for disposal via atmospheric reentry, whereas the FCC imposes a 5-year rule for the same disposal option.

None of the rules in the United States address the unique aspects of debris mitigation, flight safety, or disposal for missions that operate beyond geosynchronous orbit (GEO) [10]. However, an increasing number of actors are planning missions to the Moon, with several dozen announced to fly before the end of decade [19]. All of these missions must comply with disposal rules—there are no explicit exceptions for cislunar or lunar missions—but the rules were not designed for operations in that regime. Of particular interest is what disposal options are available to these cislunar and lunar missions. The ODMSP enumerate the disposal options for government spacecraft:

1. Direct reentry atmospheric reentry (at Earth)
2. Heliocentric Earth escape
3. Storage between LEO and GEO
4. Storage above GEO
5. Long-term reentry for structures in MEO, Tundra orbits, highly inclined GEO, and other orbits

Aside from heliocentric escape, all of the disposal options presume that a space vehicle will remain in the proximity

of Earth at end of life. For missions in cislunar space or at the Moon, the cost of returning to the Earth may be prohibitive. In the case of missions in low lunar orbit (LLO), impact on the surface of the Moon at end of life requires roughly one order of magnitude less propellant than escaping the Moon (see Section 2 below). Consequently, impact has been the preferred disposal option for mission in LLO for decades. As the number of actors in LLO expands beyond government exploration agencies to defense organizations and commercial entities, formal guidance on the safe and sustainable practice of lunar impact for disposal may become necessary.

Since the start of the space age, more than 60 vehicles have impacted the Moon. The average impact rate has been ~ 1 per year, but recent activity has increased that rate to ~ 2 per year since 2019. Most impacts have been used for disposal (controlled or uncontrolled), such as the Lunar CRater Observations and Sensing Satellite (LCROSS) [29], Lunar Atmosphere and Dust Environment Explorer (LADEE) [33], Kaguya [20], and Longjiang-2 [36]. Some of these impacts have been used to advance lunar science. The LCROSS impact, discussed in greater detail in Section 3 below, used the impact to study the chemical composition of ejecta, and Apollo ascent-stage impacts were intentionally steered into the Moon to get readings on surface seismometers [12]. Some impacts have not been intentional [8], and others have been inferred but unconfirmed, such as Apollo 11's ascent stage, which should have decayed and impacted due to lunar perturbations.

The European Space Agency (ESA) addresses lunar orbit and lunar impact in its disposal rules. ESA's Space Debris Mitigation Requirements [7] include the option that the "disposal of a spacecraft...operating in Lunar orbits shall include...lunar impact" (section 5.7.3.b of [7]) and that the "suitability of possible impact area locations on the Moon surface are analysed with respect to points of interest such as space heritage artifacts, or operational assets on the lunar surface" (section 5.7.3.c.2). No further details are provided about what metrics should be used to determine "suitability," which heritage artifacts should be protected, or what, if any, regions of the Moon should be excluded from impact.

NASA has identified some regions on the lunar surface that merit higher scrutiny for potential disturbance or contamination. NASA's planetary protection requirements classify the Moon as a Category II body [27], consistent with the Policy on Planetary Protection from the Committee on Space Research (COSPAR) [6]. Missions to the Moon must take an inventory of "organic materials, propellant residuals, and combustion products that may be released into the lunar environment" to different levels of detail depending on the destination. Missions to permanently shadowed regions (PSRs) on the Moon and the lunar poles—locations south of 79°S latitude and north of 86°N latitude—have stricter inventory requirements than those landing elsewhere. The planetary protection requirements do not prohibit operating or disposing in these regions, they only require the documentation

of potential contaminants, and these requirements only apply to NASA missions.

NASA has also developed recommendations on the preservation of sites with historical and scientific value [25]. NASA's recommendations apply to U.S. government artifacts on the lunar surface and include Apollo landing and roving hardware, unmanned landing sites (e.g., Surveyor sites), impact sites, experiments left on the lunar surface (e.g., tools, equipment, and miscellaneous hardware), and specific indicators of U.S. human and human-robotic presence, such as footprints and rover tracks. In addition to identifying sites meriting heightened protection, the recommendations provide guidance on exclusion regions to avoid disturbance. Descent and landing boundaries are defined as the "outer perimeter that establishes an exclusion radius for the approach path of any lander/spacecraft toward any USG heritage lunar site" (see section A1-3 of [25]), and similar boundaries are recommended for touchdown targeting (see section A2-3). In both cases, an exclusion radius of 2 km is recommended for heritage lander sites, and 0.5 km for heritage impact sites. Rovers are also discouraged from entering the craters of heritage impact sites. The recommendations in [25] address only landers and rovers that might visit historical sites (i.e., via soft landing) and do not provide guidance on preserving those sites from disposal impacts at high velocity. Nonetheless, NASA's recommendations imply that any exclusion zone derived for disposal impacts should be no closer than that for landers and rovers, namely 2 or 0.5 km.

2. COMPARISON OF IMPACT VS. ESCAPE FOR DISPOSAL

The two disposal options available to a spacecraft in lunar orbit at end of life are impact or escape. Leaving a derelict in lunar orbit would eventually lead to an uncontrolled impact due to orbit perturbations, but we consider here only controlled impacts targeted with a propulsive maneuver. A mission designer's choice between impact and escape depends in part on the two options' necessary ΔV , which in turn depends on the mission orbit. For escape, we include only the maneuver necessary to escape lunar orbit and neglect any subsequent disposal activity, such as returning to the Earth or effecting a heliocentric escape.

To impact the surface of the Moon, a spacecraft in an elliptical lunar orbit should perform a maneuver at aposelene that lowers periselene to the radius of the Moon, R_M , or lower. For an orbit with pre-maneuver periselene radius r_p^- and aposelene r_a , the necessary ΔV for impact is

$$\Delta V_{\text{impact}} = \sqrt{\frac{2\mu_M}{r_a}} \left(\sqrt{\frac{1}{1+\rho^-}} - \sqrt{\frac{1}{1+\rho^+}} \right), \quad (1)$$

where μ_M is the gravitational parameter of the Moon ($\sim 4,902 \text{ km}^3/\text{s}^2$) and for brevity $\rho^- \equiv r_a/r_p^-$ and $\rho^+ \equiv r_a/R_M$.

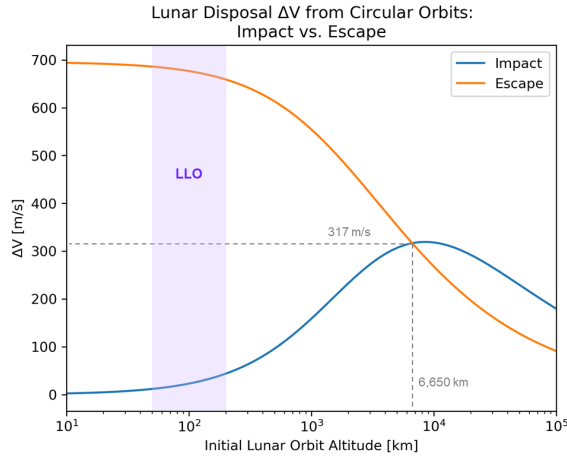


Figure 1. Disposal ΔV for impact and escape from selenocentric circular orbits as a function of initial orbit altitude.

To escape the Moon, the optimal location to perform a disposal burn is at periselene, and the ΔV for escape is

$$\Delta V_{\text{escape}} = \sqrt{\frac{2\mu_M}{r_p^-}} \left[1 - \left(1 - \frac{1}{1 + \rho^-} \right)^{1/2} \right]. \quad (2)$$

Impact is preferential to escape when $\Delta V_{\text{impact}} < \Delta V_{\text{escape}}$. After some manipulation of Eqs. 1 and 2, one finds that the condition to prefer impact over escape is

$$r_p^- < 4R_M \left(1 + \frac{R_M}{r_a} \right). \quad (3)$$

In the case of circular orbits, $r_p^- = r_a = a$, where a is the semimajor axis of the initial selenocentric circular orbit, and Eq. 3 reduces to

$$a < 2 \left(1 + \sqrt{2} \right) R_M \approx 4.828 R_M \approx 8,387 \text{ km}. \quad (4)$$

When the initial semimajor axis is less than 8,387 km—or, the initial orbit altitude is less than approximately 6,650 km—impact is preferred over escape in terms of disposal ΔV . Figure 1 shows the disposal ΔV for impact and escape, including the break-even point at 6,650 km altitude, which corresponds to a ΔV of approximately 317 m/s. Above roughly 1,000 km altitude, third-body effects from the Earth may make escape easier to accomplish than indicated by the above analysis, which uses only two-body assumptions for Keplerian orbits at the Moon. Nonetheless, many missions to the Moon operate below 1,000 km in LLO, which has no formal definition but Fig. 1 bounds between 50 and 200 km altitude. From LLO, the ΔV to impact the Moon is less than ~ 50 m/s, whereas escape would cost > 650 m/s. In terms of ΔV , impact would always be preferred over escape for missions in LLO. This order-of-magnitude disparity in ΔV cost has contributed to the historical preference for lunar missions (e.g., LADEE, Kaguya, Longjiang-2,

et al.) to use impact for disposal, and the large number of upcoming missions to the Moon that use volume- and mass-constrained form factors such as the CubeSat suggests that impact will be preferred at a large scale for the foreseeable future.

3. EFFECTS OF A LUNAR IMPACT

Whether coming from lunar orbit or from a translunar injection from Earth, a man-made space vehicle impacts the surface of the Moon with a velocity of $\sim 1\text{--}3$ km/s. (In contrast, natural impacts from micrometeoroids occur at > 10 km/s [28].) The impact excavates a crater and creates a curtain of ejecta that extends upwards and outwards from the point of impact. A typical ejecta curtain is angled $\sim 45^\circ$ to the surface [22] (see also [11] and [14]), although the curtain can take on additional components depending on the properties of the impactor. The crater from a man-made impact stays within the regolith layer, around 5–15 meters deep. The total mass of ejecta is usually 3–4 orders of magnitude higher than the impactor mass for natural impacts [1] and would be roughly an order of magnitude lower for man-made impacts due to the lower impact velocity, per the scaling of ejecta mass via power laws [17].

One of the most closely studied man-made impacts on the lunar surface was LCROSS [29]. LCROSS impacted the Moon on 9 October 2009 and consisted of two vehicles, the Centaur upper stage as the primary impactor and a trailing observer vehicle that collected data on the upper-stage impact before impacting the Moon itself 4.2 min after the Centaur. The impact occurred at an angle $85^\circ \pm 5^\circ$ from horizontal at 2.5 km/s and created a double ejecta curtain, one at $35\text{--}50^\circ$ and another at $\sim 75^\circ$. The second, high-angle curtain was due to the low-density, hollow-cylinder form of the empty Centaur [15]. The highest ejecta velocities were approximately 2,000 m/s, near escape velocity. The impact excavated a crater into the regolith < 10 m deep and 25–30 m across, and the Lunar Reconnaissance Orbiter later observed an ejecta blanket ~ 150 m across [29].

The LCROSS impact produced roughly 10^5 kg of ejecta. Pre-flight simulations predicted that the impact would produce between 200,000 [30] and 500,000 [21] kg tons of ejecta, of which 10,000–20,000 kg ($\sim 5\text{--}10\%$) of ejecta would reach an altitude sufficient for illumination by the Sun [30] and for subsequent data collection by the trailing observer vehicle. During the real-world event, 4,000–6,000 kg reached sunlight [29], implying the production of 40,000–120,000 kg of total ejecta from the impact. The Centaur’s mass was 2,350 kg, indicating that the impact produced roughly two orders of magnitude more ejecta mass than the impactor’s mass, consistent with Artemieva’s result above [1] when scaling for LCROSS’s impact velocity.

The effects of a lunar impact are transient and localized, but they are not negligible. When contemplating a lunar

impact for disposal, the resulting impact ejecta may pose the following risks:

1. **Contamination of protected regions.** The Moon has numerous geographical regions of scientific interest, such as the polar regions, where an impact and its associated ejecta could contaminate these regions with seismic, chemical, and particulate effects that prevent or impair future research. NASA's requirements for planetary protection specify latitude bounds near the lunar poles that warrant heightened vigilance for any missions destined to visit there [27]. Article IX of the Outer Space Treaty requires signatory parties exploring celestial bodies such as the Moon to "avoid their harmful contamination" [34].
2. **Damage to nearby assets.** Impact ejecta consists of regolith particles moving at high speed that subsequently return to the surface of the Moon some distance away. The re-impact of the ejecta could damage or injure nearby manned or robotic assets on the surface, including active missions and historical sites of interest. The Apollo 12 mission landed 180 meters from the Surveyor III lander, kicking up large amounts of ejecta from the lunar module's main engine. During a moonwalk, astronaut Charles Conrad approached the lander and found "the surface of the Surveyor III craft was scoured and pitted by the ejected regolith." [18]
3. **Danger to other orbital vehicles.** Impact ejecta can reach the altitudes of other spacecraft orbiting the Moon, and the ejecta particles may pose a penetration risk to sensitive surfaces and systems. Lunar-surface launches also kick up ejecta that poses a risk of pitting and ablation to vehicles in lunar orbit, such as the Lunar Gateway. [23]
4. **Anthropogenic effects to the lunar exosphere.** Natural impactors (i.e., micrometeoroids) and subsequent ejecta "provide a significant source for the rarefied lunar atmosphere." [28] Man-made impacts would both inject more regolith ejecta into the lunar exosphere and introduce new species, such as aluminum particles, that may affect science of the Moon's and Solar System's evolution. Some scientists have already called for the declaration of a new geological era for the Moon due to human impacts on the environment there. [16]

This paper focuses on item 2 above. A man-made impact that disposes of a derelict from LLO poses a risk to nearby assets from both the impact itself and the resulting ejecta curtain. If impact were to become a more common occurrence for disposal, the community would benefit from clearer guidance on how to reduce this risk by observing exclusion regions around protected sites.

This paper investigates the sizing of an impact-exclusion range near protected sites on the lunar surface. The appropriate range depends on the risk tolerance for protected assets, which may vary across different actors and

assets. The space-debris community has defined risk thresholds in other domains and applications, such as the probability of collision with manned and unmanned assets in low Earth orbit and reentry-casualty risk. For example, the ODMSP use a 10^{-3} probability of collision with large objects over 100 years and a 10^{-4} casualty risk for objects reentering the Earth's atmosphere and surviving to impact the surface [35]. Risk thresholds for assets on the lunar surface remain undefined. Nonetheless, the extant examples indicate that the driving metric for damage or injury risk is the kinetic energy of a colliding particle. In the context of disposal via lunar impact, this metric corresponds to the kinetic energy of impact-ejecta particles at range and those particles' probability of penetration of protected assets.

To arrive at a recommendation on an impact-exclusion range, this analysis proceeds in three steps:

1. Assess how much ejecta is created by an impact, where it goes, and how much kinetic energy it has as a function of range from the impact site.
2. Propose kinetic energy levels to use as thresholds for damage or injury.
3. Determine the probability of damage or injury as a function of kinetic-energy threshold and range, and recommend a limiting range based on historical thresholds for tolerable damage and injury probabilities.

4. DYNAMICS AND PROPERTIES OF EJECTA FROM A MAN-MADE IMPACT

The range R of a ballistic projectile such as impact ejecta depends on the ejection velocity v and flight path angle β ,

$$\tan \frac{R}{2R_M} = \frac{-(Q/2) \sin 2\beta}{Q \cos^2 \beta - 1}, \quad (5)$$

where $Q \equiv v^2 R_M / \mu_M$ [2]. The flight path angle of ejecta from a typical impact is approximately $\beta = \pi/4$ (i.e., 45°). This ejection angle also maximizes the range up to $Q \leq 1/2$ (~ 1.1 km/s at the Moon), which is also near the upper limit of ejecta velocity from man-made impacts. Figure 2 shows the range of impact ejecta as a function of ejection velocity for ejection angles of 30° , 45° , and 60° . As expected, the range is maximized for a launch angle of 45° (orange in Fig. 2) until the launch velocity is ~ 1.1 km/s. Below ~ 700 m/s ejection velocity and ~ 300 km range, the range varies by less than 10% between these three ejection angles. Conclusions drawn for the nominal case of $\beta = 45^\circ$ should therefore roughly hold for a range of ejection angles observed in historical impacts, such as the 35 – 50° range observed for the primary ejecta curtain of the LCROSS impact, as noted above.

The kinetic energy of an ejecta particle depends on its velocity, which one can solve for by inverting Eq. 5. Setting

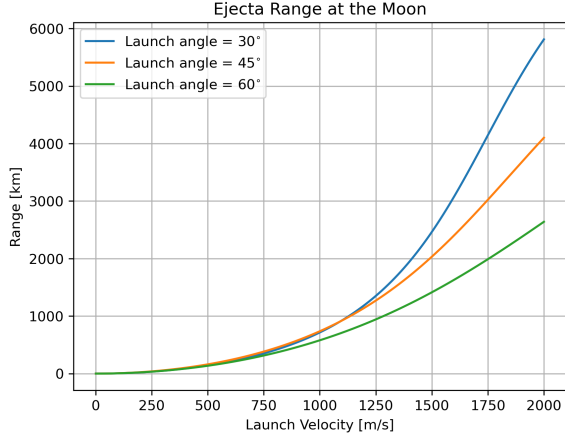


Figure 2. Ejecta range from a lunar impact as a function of ejection velocity for three different ejection angles. The range is insensitive to ejection angles between 30° and 60° except at the highest ejection velocities, varying less than 10% up to ~ 700 m/s and ~ 300 km range.

$\beta = \pi/4$ for a nominal impact-ejecta curtain yields

$$v(R) = \sqrt{\frac{2\mu_M/R_M}{1 + \cot(R/2R_M)}}. \quad (6)$$

The properties of the impact ejecta can be estimated following the model developed by Housen & Holsapple [17]. The total mass of ejecta M moving faster than velocity v is given in Table 1 of [17] as

$$M(v) = mC_4 \left[\frac{v}{U} \left(\frac{\rho}{\delta} \right)^{(3\nu-1)/3\mu} \right]^{-3\mu}, \quad (7)$$

where m is the mass of the original impactor, U is the impactor velocity, ρ the density of the target (i.e., lunar regolith), δ the density of the impactor, and C_4 , ν , and μ are constants that depend on the properties of the lunar regolith. Substitution of Eq. 6 would yield $M(R)$, but $M(R)$ is a cumulative distribution for the total ejecta mass at range *greater than* R . An alternative property of the ejecta curtain that is not cumulative, the areal mass density σ at range, can be derived from Eq. 7,

$$\begin{aligned} \sigma(R) &= -\frac{1}{2\pi R} \frac{dM(R)}{dR} \\ &= \frac{3\mu K}{16\pi\mu_M} \frac{v(R)^{-3\mu+2}}{R} \csc^2\left(\frac{R}{2R_M}\right), \end{aligned} \quad (8)$$

where $K \equiv mC_4U^{3\mu}(\rho/\delta)^{1-3\nu}$. The areal density will be a direct input later into the equation for the probability of damage or injury.

Equations 7 and 8 include several constants that depend on the properties of the target material that the impactor strikes. Table 3 of [17] provides values for these constants for a variety of different materials based on published data, mostly from impact experimentation in a lab.

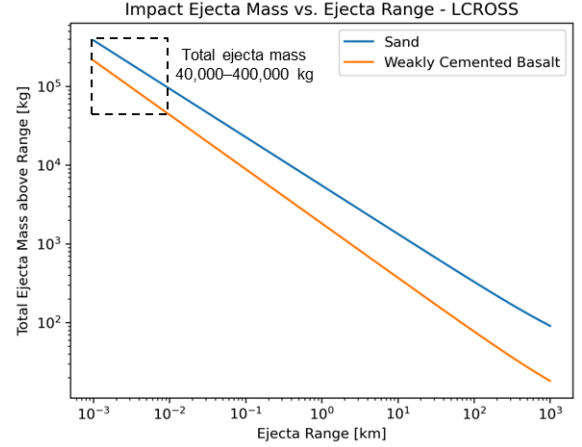


Figure 3. Prediction of LCROSS impact-ejecta mass vs. range using the model from [17]. The model predicts a total ejecta mass of 40,000–400,000 kg depending on the properties of the regolith-like target material, consistent with the ejecta mass observed from the real-world LCROSS impact in 2009.

Unfortunately, lunar regolith is not among the target materials. The options in [17] that most closely resemble regolith and that roughly bound regolith's properties are sand and weakly cemented basalt (WSB). Table 1 lists the porosity and bulk density of WCB and Sand from [17] with a qualitative description of each and compares them to the same properties for lunar regolith, based on formulae supplied in Section 9.1.4 of [13] and other data supplied elsewhere from that reference. Both WCB and sand were tested with sub-hypervelocity impacts comparable to man-made impact velocities. The porosity and bulk density of sand is most comparable to regolith, but the density of WCB may more closely reflect the density of individual regolith particles, compacted regolith, and breccias. This analysis uses both target models going forward.

This paper's ejecta model for lunar impacts developed from [17] reproduces the results from the LCROSS impact. As described above, the impact of the LCROSS Centaur upper stage excavated a crater 25–30 meters across and produced roughly 10^5 kg of ejecta. Figure 3 shows a plot of the predicted ejecta mass from this paper's impact-ejecta model, using the physical properties of LCROSS from [29]. The plot shows the predicted cumulative mass as a function of range, so the values at the far left of the plot indicate the total ejecta mass from the impact. The model predicts the LCROSS impact would produce 40,000–400,000 kg of ejecta, which is consistent with both the pre-flight predictions and the observed amount during the real-world impact event. Furthermore, Table 1 of [17] provides equations for modeling the size of the impact crater. Again using the properties of the LCROSS Centaur upper stage, this model predicts a crater size between 12 m in the gravity regime (i.e., the sand target) and 72 m in the strength regime (i.e., WCB target), which bounds the observed crater. The con-

Table 1. Comparison between Regolith-Like Impact Targets and Lunar Regolith

	Housen & Holsapple [17], Table 3		Lunar Regolith [13]
Target	WCB	Sand	
Porosity	20%	35 ± 5%	40–50%
Bulk Density	2,600 kg/m ³	1,600 kg/m ³	1,300–1,900 kg/m ³
Description	“1900 m/s impacts into weakly cemented basalt consisting of mm-size crushed basalt fragments, iron grit, and fly ash as a binding agent.”	“Impacts of...aluminum sphere into the 1–3 mm fraction of commercial blasting sand. The impact speed ranged from 800 to 1900 m/s.”	

sistency between the model predictions and the observed LCROSS impact properties suggests that the model can faithfully bound the ejecta behavior and bulk properties for the man-made impacts considered in this analysis.

Calculating the kinetic energy of ejecta particles requires knowing their mass and velocity at range. However, the ejecta model only provides the bulk properties of the ejecta curtain, namely the *total mass* beyond range R (i.e., $M[v(R)]$ per Eqs. 6 and 7) or the areal mass density at range R (i.e., $\sigma(R)$ per Eq. 8). The distribution of the ejecta particle size and mass at range (or vs. ejection velocity) is unknown, and the literature on impact-ejecta modeling does not appear to provide formulae for modeling these distributions [REF]. Consequently, this analysis makes a conservative “critical particle” assumption: for a specific kinetic-energy threshold KE^* , all ejecta particles at range R have a mass m^* so that

$$KE^* = (1/2)m^*v(R)^2 . \quad (9)$$

This assumption implies that every ejecta particle is massive enough to violate the kinetic-energy threshold (e.g., to penetrate a protected asset). This conservative assumption should maximize the overall risk in the analysis. If the ejecta particles were more massive (i.e., greater than m^*), they would still violate the kinetic-energy threshold, but there would be fewer of them (assuming a fixed total ejecta mass from the bulk properties calculated in the ejecta model), reducing the risk. If the ejecta particles were less massive, they would no longer violate the kinetic-energy threshold and no longer present a risk.

All together, it is possible to express the probability of damage or injury at range R via the areal mass density, critical-particle mass, and exposed area of the protected asset, A ,

$$P_{\text{damage}} = 1 - e^{-\sigma(R)A/m^*(R)} . \quad (10)$$

5. KINETIC ENERGY THRESHOLDS

5.1. Penetration of Habitats and Robotic Assets

The penetration of habitats or robotic assets depends on both an impacting ejecta-particle’s size and its kinetic en-

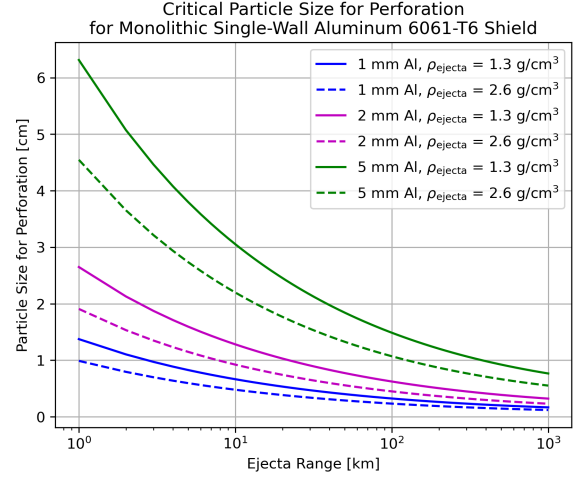


Figure 4. Diameter of particles that perforate protected assets as a function of range from the disposal impact site, for varying aluminum-shielding thickness and ejecta-particle densities.

ergy. For simplicity, we assume that habitats and robotic assets are made of plate aluminum (or the equivalent thickness of plate aluminum). A formula for the perforating particle size is given by [4] (see section 4.1.1 therein) in terms of the particle’s impact velocity and properties of the ejecta particle and protected asset, such as the objects’ densities, speed of sound, and hardness. Using the appropriate values for aluminum, Fig. 4 shows the particle sizes to perforate a protected asset as a function of range from the original disposal impact site. These plots represent classic ballistic limit curves but with the velocity on the horizontal axis replaced by the derived range. Figure 4 considered 1–5 mm of aluminum shielding and two different ejecta densities and assumed that the ejecta impact is normal to the surface of the protected asset, which is the most conservative condition for penetration. Perforating particle diameters range from ~1 mm at the furthest ranges to >1 cm at ranges less than 1 km.

The particle sizes of Fig. 4 can be replaced with equivalent kinetic energy, as shown in Fig. 5. The kinetic energy of a perforating particle is insensitive to both range and ejecta-particle density and most sensitive to the thickness of the aluminum shielding. Consequently, a sin-

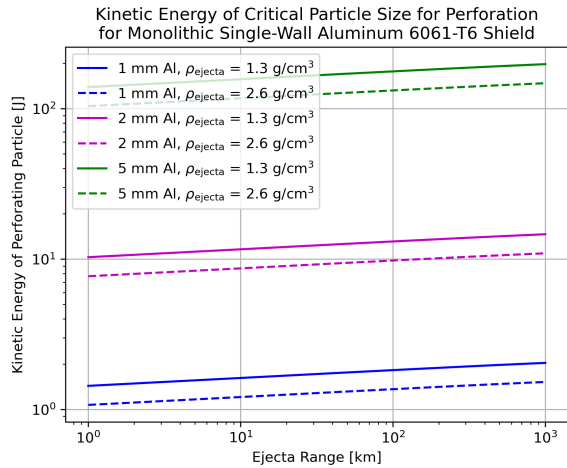


Figure 5. Kinetic energy of particles that perforate protected assets as a function of range from the disposal impact site, for varying aluminum-shielding thickness and ejecta-particle densities.

Table 2. Kinetic-Energy Thresholds for Penetrating Habitats and Robotic Assets

Limits	Threshold [J]	Note
Robotic	~10	~2 mm Al
Habitat	>150	>5 mm Al

gle kinetic-energy threshold should be adequate for any given protected asset, depending on its level of shielding. For manned habitats, protection from micrometeoroids and debris is provided by Whipple shields that “consist of an outer bumper (typically aluminum), multi-layer insulation (MLI) thermal blanket, and an inner rear-wall or pressure shell (also aluminum typically)” [4]. These shields provide protection equivalent to >5 cm of plate aluminum at the ejecta-impact velocities considered here (<1 km/s). Figure 5 therefore suggests using a kinetic-energy threshold of 150 J or greater for a manned habitat.¹ For robotic assets, the literature indicates that Mars rovers have shielding of 1.5–2.25 mm of plate aluminum [9], and the Intuitive Machines lunar lander IM-1 had shielding ranging from 1–5 mm depending on the intervening components [24]. If ~2 mm of aluminum is a reasonable assumption for the protection of robotic assets, Fig. 5 indicates a kinetic-energy threshold of ~10 J is appropriate. Table 2 summarizes the kinetic-energy thresholds used in this analysis to penetrate robotic and habitat protected assets.

¹Calculating the ballistic limit curves developed in [4] explicitly for Whipple shields on the International Space Station (ISS) yields penetrating kinetic energies of 200–300 J for particles impacting at ~1 km/s, consistent with assumption for this analysis to use a conservative threshold of 150 J.

Table 3. Kinetic-Energy Thresholds for Injury to Humans

Limits	Threshold [J]
Spacesuit bladder penetration	3
Casualty for unprotected human	15
Uncontrollable spacesuit leak	56
>90% probability of fatality for unprotected human	>115 J

5.2. Injury to Humans on the Lunar Surface

The danger posed to humans on the lunar surface from impact ejecta depends on the level of protection. The terrestrial “casualty” threshold used for reentry analysis at Earth—that is, for an *unprotected* human—is 15 J [26]. This value derives from the “injury” threshold in [5], which also identifies a 50% fatality threshold of 58 ft·lbf (78.6 J) and 90% fatality at 85 ft·lbf (115.2 J) for an unprotected human.

Humans on the lunar surface will be protected by at least a spacesuit, which has an alternative set of penetration-energy thresholds. Penetrating a spacesuit bladder occurs at ~3 J [3]. Penetration at this energy level would trigger a leak and termination of any ongoing moonwalk activity, but the leak would not be catastrophic. Per [3], “Oxygen pressure is regulated to maintain suit pressure at safe levels for a minimum of 30 minutes with holes up to 4 mm in diameter.” With a penetration at 3 J, the astronaut would have 30 minutes to return to safety without direct injury. Christiansen [3] indicates an uncontrollable leak would be triggered at 56 J, and the hard components of a spacesuit would be penetrated from 3.5–71 J. Table 3 summarizes the kinetic-energy thresholds used in this analysis for injury to humans on the lunar surface.

5.3. Realism of Critical-Particle Sizes

An ejecta particle that poses a risk of damage or injury must not only have sufficient kinetic energy to penetrate a protected asset but also be a size expected to be found in lunar regolith. Figure 6 shows the diameter of “critical particles” as a function of range from the impact site. The critical-particle diameters are plotted for different impacting kinetic energies (3, 50, and 150 J) and different ejecta-particle densities, using the densities of sand and WCB from [17] and Tab. 1. For ranges between 1 and 100 km, the diameters of critical particles range from roughly 1 mm to ~4–6 cm. Comparison between Figs. 4 and 6 show that the perforating particle sizes are consistent with the critical-particle diameters.

These critical-particle sizes are consistent with or slightly larger than regolith samples from the lunar surface and regolith simulants. The JSC-1A regolith simulant consists of >95% of particles <1 mm in size [39], and the lunar-

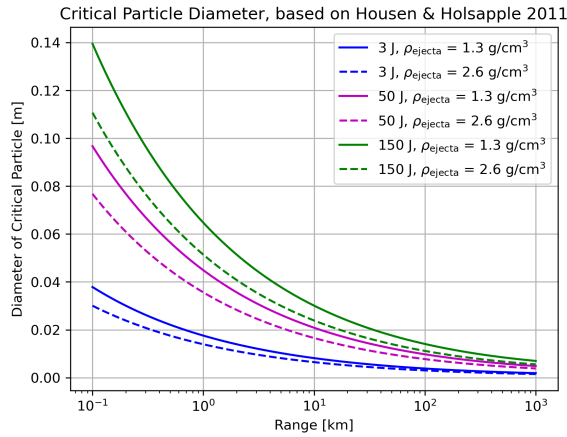


Figure 6. Diameter of critical particles as a function of range from the impact site. These sizes are consistent with particles found in lunar regolith.

soil average collected from manned missions to the Moon consisted of $\sim 90\%$ of particles < 1 mm in size and some larger than 2 cm (see Figs. 7.9 and 7.29 in [13]). Apollo samples contained no regolith particles greater than 3 cm. However, other rocks and breccia—either already present or fractured during impact—could be larger. As noted in [25], “Careful review of the [Apollo 11] landing videos, and comparison to plume modeling, shows that gravel and rocks 1 cm to 10 cm in diameter were also ejected by the plume at speeds between 5 and 50 m/s. Ballistic calculation indicates that these rocks impacted the lunar surface up to 1.5 km from the LM.”

These historical data of regolith composition in conjunction with Fig. 6 indicate that using a “critical particle” is a conservative choice. Within ~ 1 km of the impact site, critical particles that have high kinetic energy (e.g., 50–150 J) may not be particularly abundant in the ejecta curtain, but this analysis would assume that all the particles have that size. Even at > 10 km range, critical-particle diameters are roughly 1 mm in size, which appear to make up less than 10% of typical regolith particles. It is not clear if or how many particles at cm-scale would be ejected fast enough to reach 10+ km range (> 200 m/s ejection velocity). Consequently, the critical-particle assumption may be conservative by roughly one order of magnitude. This conservatism will be incorporated later in the downselection of a recommended keep-out zone.

6. PROBABILITY OF DAMAGE OR INJURY

The probability of damage or injury can be calculated via Eq. 10, using the energy thresholds of Tabs. 2 and 3 to determine the critical particle mass m^* per Eq. 9.

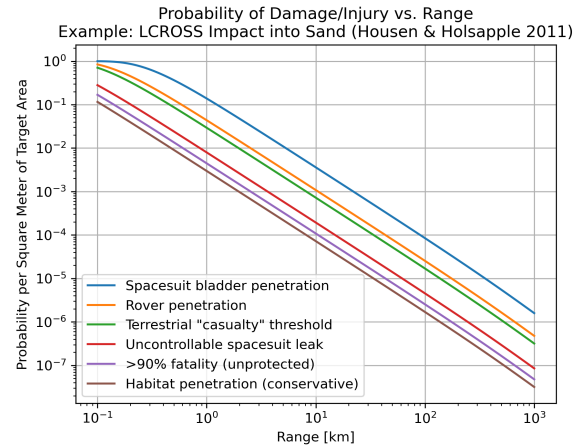


Figure 7. Probability of damage or injury per square meter of target area for the LCROSS impact into sand [17] as a function of range from the LCROSS impact site.

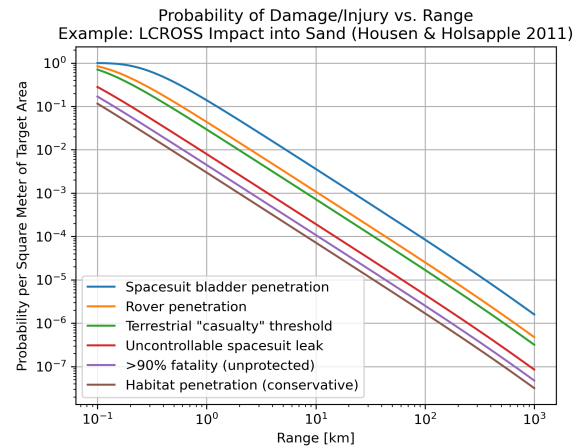


Figure 8. Probability of damage or injury per square meter of target area for the LCROSS impact into WCB [17] as a function of range from the LCROSS impact site.

6.1. Examples for LCROSS and LRO

Figures 7 and 8 show the probabilities of damage or injury per square meter of target area for the LCROSS impact into sand and WCB, respectively, as a function of range from the LCROSS impact site. Humans and rovers have a cross-section of approximately 1 m^2 , but habitats may be 10–100 times larger. Depending on the kinetic-energy threshold, $P_{\text{damage}} = 10^{-4}$ at ~ 5 –100 km range. Within one kilometer range, the probability of spacesuit bladder penetration is $> 10\%$, highlighting the hazard to any human presence in the vicinity of a man-made impact. The WCB case shifts the probability down by approximately one order of magnitude. The risk for high kinetic-energy cases (e.g., “habitat penetration” at 150 J) at < 10 km range is overstated. The threshold penetrating particles for these cases must be > 4 cm, which exceed recorded regolith particle sizes.

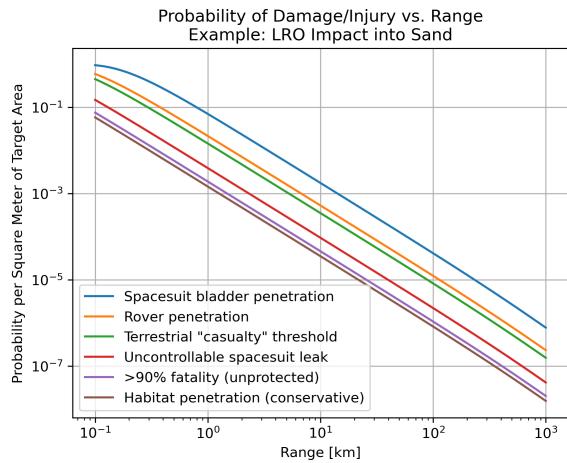


Figure 9. Probability of damage or injury per square meter of target area for a notional LRO impact into sand [17] as a function of range from the LRO impact site.

LCROSS's impact was notable for the unusual properties of the hollow Centaur upper stage impactor: a very low density (25 kg/m^3) and high impact velocity ($2,500 \text{ m/s}$). In contrast, the notional disposal of the Lunar Reconnaissance Orbiter (LRO) via lunar impact may be more representative of future impacts. If we assume that LRO, with a dry mass of $1,018 \text{ kg}$ and bus density of $\sim 500 \text{ kg/m}^3$, will use propulsion to lower periselene to a sub-surface altitude, it would have an impact velocity of $\sim 1,700 \text{ m/s}$. Figure 9 shows a plot of probability of damage or injury for this notional LRO impact into sand. For brevity, the case with WCB is not shown. As with LCROSS, an impact into WCB reduces the probability of damage by nearly one order of magnitude. The lower impact velocity and lower impactor mass of LRO compared to LCROSS shifts the curves to left. That is, LRO's less energetic impact does not send ejecta as far across all kinetic-energy thresholds.

6.2. Risk Across Different Potential Impactors

Impactor properties will vary widely in the real world, including both large and small spacecraft from different pre-impact operational orbits that affect the impact velocity on the lunar surface. Section 6.1 explored the risk for two point cases, LCROSS and LRO. To develop a recommendation for an overall impact keep-out zone, it is necessary to vary the impactor mass, density, and velocity across a range of credible values in a Monte Carlo fashion. The objective of the analysis is to find the furthest range that violates a given kinetic-energy penetration threshold at a specific level of P_{damage} . This analysis uses uniform distributions to identify the upper bounds of range. Table 4 shows the range of impactor parameters used in the Monte Carlo runs. Figure 10 shows an example histogram of ejecta impact ranges, for a specific kinetic-energy threshold (10 J) and P_{damage} (10^{-4}). To

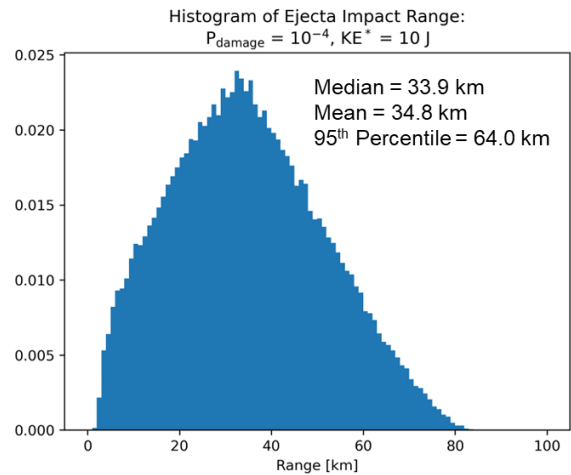


Figure 10. Example histogram of ejecta impact ranges for a particular kinetic-energy threshold and P_{damage} .

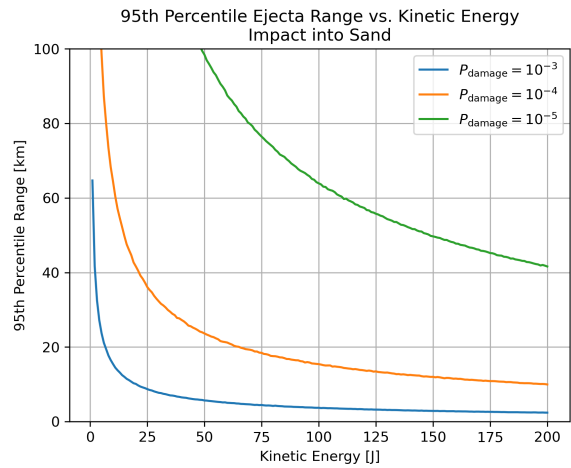


Figure 11. 95th percentile range of ejecta as a function of kinetic-energy threshold, for several contours of probability of damage or injury (per square meter of target area), using sand as the analogue for lunar regolith.

avoid statistical instability in the maximum of the range distributions, this analysis will use the 95th percentile value as the relevant metric.

For each Monte Carlo run, which corresponds to a stochastic variation across spacecraft-impactor properties, the 95th percentile range is recorded for a given kinetic-energy threshold and P_{damage} (per unit area of the protected asset). This analysis is repeated twice for the two impact materials, sand and WCB. Figures 11 and 12 show the 95th percentile ejecta range as a function of kinetic-energy threshold for different levels of P_{damage} from 10^{-3} to 10^{-5} . Figure 11 shows the ejecta range for a spacecraft impact into sand as an analogue for lunar regolith, and Fig. 12 shows the same results for impact into WCB. These two figures provide the necessary insight to select an appropriate keep-out zone size for impact via disposal, given a risk tolerance (P_{damage}) and vul-

Table 4. Impactor Parameters Varied in Monte-Carlo Analysis

Model Variable	Range	Distribution	Notes
Impactor Mass	25–3,000 kg	Uniform	Low end: smallest lunar orbiters (e.g., CAPSTONE) High end: large upper stages and s/c buses
Impactor Density	25–500 kg/m ³	Uniform	Low end: hollow LCROSS Centaur upper stage High end: densest large buses
Impact Velocity	1-3 km/s	Uniform	Low end: large disposal ΔV from LLO High end: TLI-like impact velocity

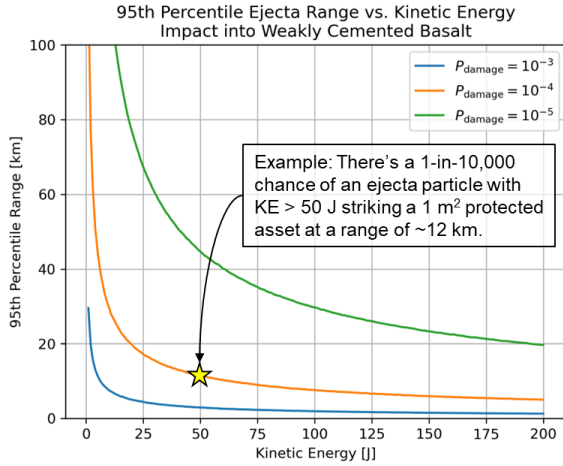


Figure 12. 95th percentile range of ejecta as a function of kinetic-energy threshold, for several contours of probability of damage or injury (per square meter of target area), using WCB as the analogue for lunar regolith.

nerability (kinetic-energy threshold). Figure 12 includes an annotated example for impact into WCB: for a protected asset vulnerable to a particle with 50 J of kinetic energy and where the desired probability of penetration P_{damage} (per unit area) is 10^{-4} (or less), then man-made impactors should impact ~ 12 km from that asset or farther.

7. DOWN-SELECTION AND RECOMMENDATION ON LUNAR-IMPACT EXCLUSION REGION

Sufficient data are now available to develop a recommendation on the size of a lunar-impact exclusion region. Figures 11 and 12 provide the relationship between extremal impact-ejecta range, kinetic energy of the penetrating ejecta particles, and the risk tolerance of a protected asset, P_{damage} . Tables 2 and 3 provide kinetic-energy thresholds for penetrating protected assets or injuring humans on the lunar surface. Combining these two resources yields Tab. 5, which shows the extremal (95th percentile) ejecta range for specific kinetic-energy thresh-

olds and risk tolerances. Some scaling observations are worth noting. Reducing P_{damage} by one order of magnitude increases the range by a factor of ~ 4 , and increasing the kinetic-energy threshold by an order of magnitude reduces the range by a similar amount. The ranges in Tab. 5 for impact into sand are roughly two times greater than for impact into WCB. These scaling behaviors of the ejecta range are a result of the analytical ejecta model based on [17],

$$\text{Ejecta Range} \propto \left(\frac{1}{\text{KE} * P_{\text{damage}}} \right)^\alpha, \quad (11)$$

where $\alpha = 0.41$ for sand and 0.46 for WCB.

Downselecting to a specific recommendation from Tab. 5 requires consideration of several factors related to the risk tolerance of protected assets. The following considerations were included for a final down-selection:

- The ODMSP use 10^{-4} as a threshold for casualty probability from vehicles reentering the Earth's atmosphere [35], indicating a consensus value for the risk that could or should be applied to humans from spaceflight activities. For ejecta-related risk to humans on the lunar surface, it therefore may be reasonable to start with $P_{\text{damage}} \leq 10^{-4}$.

Action: Remove $P_{\text{damage}} \geq 10^{-5}$ from Tab. 5 for human-related risks.

- Humans will never be unprotected on the lunar surface. Spacesuit layers are likely to reduce effective casualty probability by one (or more) orders of magnitude for a given kinetic energy [5]. Cole (Fig. 2.9 in [5]) shows how curves for probability of penetration shift for additional layers of clothing. For example, going from bare skin to 6 clothing layers, which a spacesuit may resemble in protection, reduces the probability of penetration from $\sim 95\%$ to $\sim 5\%$, roughly an order of magnitude. If this analysis is benchmarking $P_{\text{damage}} \leq 10^{-4}$ for *unprotected* human casualty probability, it may be reasonable to use 10^{-3} (or higher) as an effective threshold at same energy levels for humans in a spacesuit.

Action: Remove $P_{\text{damage}} = 10^{-4}$ for *unprotected* human cases in Tab. 5, as the effective P_{damage} is $\sim 10^{-3}$.

Table 5. Extremal Ejecta Ranges for a Man-Made Impactor on the Lunar Surface

95 th Percentile Ejecta Range		P_{damage} (Impact into Sand)			P_{damage} (Impact into WCB)		
Damage / Injury	Kinetic Energy [J]	10^{-3}	10^{-4}	10^{-5}	10^{-3}	10^{-4}	10^{-5}
Spacesuit bladder penetration	3	32.2 km	135.9 km	560.0 km	15.5 km	60.2 km	236.2 km
Rover penetration (conservative)	10	15.4 km	64.5 km	266.6 km	7.7 km	29.9 km	115.9 km
Terrestrial “casualty” threshold	15	12.0 km	49.7 km	207.4 km	6.0 km	23.4 km	91.0 km
Uncontrollable spacesuit leak	56	5.3 km	22.1 km	91.8 km	2.7 km	10.7 km	41.8 km
>90% fatality (unprotected)	115	3.4 km	14.0 km	58.8 km	1.8 km	7.0 km	27.4 km
Habitat penetration (conservative)	150	2.9 km	12.0 km	49.7 km	1.5 km	6.0 km	23.4 km

- The spacesuit bladder-penetration threshold (3 J) does not imply immediate (or any) casualty. The spacesuits assessed in [3] were designed to provide >30 min of oxygen for holes <4 mm in size. Using 3 J as a cutoff for the exclusion range may be overly conservative.

Action: Remove the 3 J (spacesuit bladder penetration) case as overly conservative.

- For robotic orbiters, the ODMSP accept collision-risk probabilities of 10^{-2} (against small debris over the mission life) and 10^{-3} (against large objects over 100 years). It may therefore be reasonable to use $P_{\text{damage}} \leq 10^{-3}$ (or even 10^{-2}) for risk to unmanned assets on the lunar surface.

Action: For unmanned protected assets (e.g., “rover penetration”), remove cases for $P_{\text{damage}} \leq 10^{-4}$.

Taking each of the actions listed above to eliminate unduly conservative ranges yields the remaining table in Tab. 6, where removed cases are marked with a strikethrough. Among the remaining cases, the greatest range is 22.1 km, corresponding to an uncontrollable spacesuit leak (56 J) at $P_{\text{damage}} = 10^{-4}$. Figure 6 indicates that the critical-particle diameter at this range and kinetic energy is approximately 1.5 cm, which is an observed particle size in lunar regolith (see section 5) and therefore cannot be immediately dismissed as unrealistic as a penetration threat. Given the myriad assumptions and layers of conservatism applied throughout this analysis, and given the preference for a round number that can be used in policy or requirements, we recommend rounding the size of the keep-out region to 20 km.

8. CONSERVATISM IN SIZING THE KEEP-OUT REGION

This analysis has made several assumptions that introduce conservatism into the recommendation of 20 km for

the size of the keep-out region. The analysis assumed that all ejecta mass at range is made up of “critical-sized” particles that achieve a particular kinetic-energy threshold. Based on observed distribution of particles in lunar regolith, this assumption may be an overstatement of the count of critical-sized particles by an order of magnitude or more, particularly at ranges beyond 10 km, where the critical particles are 1–3 cm in size and constitute a small fraction of the lunar regolith. Furthermore, the recommendation used the 95th percentile range, varied across credible impactor parameters. The 95th percentile selects for the riskiest impacting vehicles with a high impact velocity (3 km/s), high mass (3,000 kg), and high density (500 kg/m^3), which may not be realistic for the vast majority of missions.

The analysis also assumed that all impacts are normal to the lunar surface. This assumption was true for the LCROSS impact and is consistent with most lab tests in the experimental literature, but it is not necessarily true for impacts from LLO. Lowering periselene to 10–100 km below the lunar surface from a circular orbit in LLO yields impact angles of $\sim 1\text{--}4^\circ$ above local horizontal, almost tangential to the lunar surface. To address a non-normal impact, Housen & Holsapple [17] suggest using the component of the impact velocity normal to the surface, “...for oblique impacts, more high-speed ejecta will be launched down-stream...many of the late-stage results such as the final crater size and shape become simply related to the normal component of the impact angle.” Some investigations have shown that the bulk properties of impact ejecta are insensitive to impact angles greater than 45° for hypervelocity impacts [37], but little experimental data appears to be available for sub-hypervelocity impacts at impact angles below 30° . If one uses the Housen & Holsapple recommendation, a grazing disposal impact from LLO might have an effective impact velocity of 30–120 m/s, and the total ejecta mass used in this analysis might be overstated by one or more orders of magnitude. However, more ejecta may be launched down-range in the direction of the impact velocity vector [32]. If so, more research may be necessary to characterize the asymmetric distribution of ejecta curtains for oblique impacts

Table 6. Extremal Ejecta Ranges for a Man-Made Impactor with Down-Selections

95 th Percentile Ejecta Range		P_{damage} (Impact into Sand)			P_{damage} (Impact into WCB)		
Damage / Injury	Kinetic Energy [J]	10^{-3}	10^{-4}	10^{-5}	10^{-3}	10^{-4}	10^{-5}
Spacesuit bladder penetration	3	32.2 km	135.9 km	560.0 km	15.5 km	60.2 km	236.2 km
Rover penetration (conservative)	10	15.4 km	64.5 km	266.6 km	7.7 km	29.9 km	115.9 km
Terrestrial “casualty” threshold	15	12.0 km	49.7 km	207.4 km	6.0 km	23.4 km	91.0 km
Uncontrollable spacesuit leak	56	5.3 km	22.1 km	91.8 km	2.7 km	10.7 km	41.8 km
>90% fatality (unprotected)	115	3.4 km	14.0 km	58.8 km	1.8 km	7.0 km	27.4 km
Habitat penetration (conservative)	150	2.9 km	12.0 km	49.7 km	1.5 km	6.0 km	23.4 km

and to revisit the appropriateness of a single keep-out radius for impact planning.

Even with this conservatism, the recommended size for the impact exclusion region has a small effect on the availability of the lunar surface for disposal via impact. We consider two sets of protected regions: 1) the lunar poles north of 86°N latitude and south of 79°S latitude per NASA’s planetary protection requirements [27], and 2) sites of historical interest that would be subject to this paper’s recommended 20-km keep-out region, which corresponds to $1,257\text{ km}^2$ per site. Figure 13 shows how the size of the impact exclusion region affects the total amount of lunar surface available for disposal by impact. Including the polar exclusion regions, the plot shows the percentage of the lunar surface available for impact for different numbers of protected sites. NASA recommends protecting all sites [25], including landers and historical impact sites, but only formally addresses U.S. sites on the lunar surface. Expanding that standard to all current and historical actors at the Moon amounts to ~ 90 sites from 1959–2023. With that most encompassing rule for protected sites, 90 sites with a keep-out region of 20 km would exclude $<2\%$ of the lunar surface, leaving $>98\%$ for impact. There may be future calls for the designation of other large regions of the lunar surface as impact keep-out regions (e.g., for scientific preservation), and an additional best practice for planning an impact would be to consult the scientific community on regions that may be more sensitive than others to the effects of an impact. In the current regime where no such *formal* restrictions exist uniformly and where informal restrictions may exist at the organizational level (e.g., applied only to NASA missions), this analysis shows that the recommended size of the keep-out zone does not unduly burden missions from finding a location to dispose via impact.

9. CONCLUSION

The growing number of actors at the Moon may warrant updates to national and international debris-mitigation

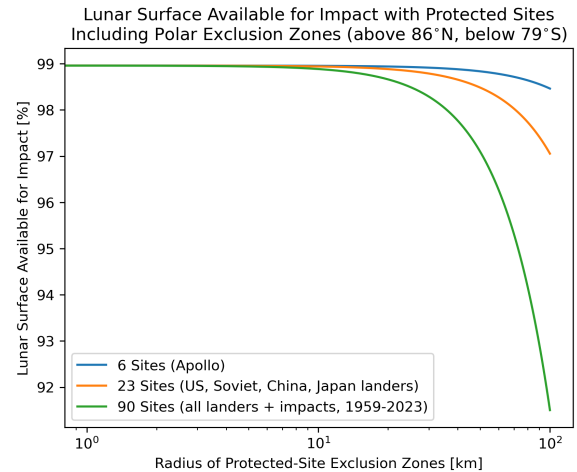


Figure 13. Fraction of the lunar surface available for disposal by impact as a function of exclusion-region size around protected sites and including the polar exclusion zones from NASA’s Planetary Protection Requirements. Imposing the recommended 20-km exclusion region to all lander and impact sites on the surface to date would leave $>98\%$ of the lunar surface available for impact.

and disposal rules in the near future, including the potential addition of a disposal option of lunar impact. If these actors embrace impact for disposal and the rate of impacts increases beyond the historical rate of once or twice per year, specific guidance may be warranted on the manner of performing an impact and where and how to protect valuable sites on the Moon. We have combined a model of the ejecta produced by man-made impacts, an estimate of the kinetic energy of the ejecta particles as a function of range, an evaluation of threshold kinetic energies that may damage or injure protected assets, and a review of risk tolerance in analogous environments (e.g., probability of casualty or collision at the Earth). We conclude that an impact-exclusion radius of 20 km around protected sites yields a level of risk consistent with that adopted in other standards, such as the ODMSP, and incorporates conservatism in several underlying assumptions throughout the analysis. A radius of 20 km is further than the only other recommendation found in the literature (2 km), which was developed for descent and landing and not impacts [25]. This larger radius does not unduly burden the use of impact as a disposal option: even accounting for 90 historical protected sites on the surface and the exclusion of the lunar poles per NASA's planetary protection recommendations, more than 98% of the Moon's surface remains available for disposal.

REFERENCES

1. Artemieva, N.A. and Shuvalov, V.V., "Numerical Simulation of High-Velocity Impact Ejecta Following Falls of Comets and Asteroids on the Moon," *Solar System Research*, 42.4 (2008): 329–334.
2. Bate, R.R., Mueller, D.D., and White, J.E., *Fundamentals of Astrodynamics*, Dover Publications, New York, 1971.
3. Christiansen, E.L., Cour-Palais, B.G., and Friesen, L.J., "Extravehicular Activity Suite Penetration Resistance," *International Journal of Impact Engineering*, 23 (1999): 113–124.
4. Christiansen, E.L., et al., "Handbook for Designing MMOD Protection," National Aeronautics & Space Administration, JSC-64399, 2009.
5. Cole, J.K., Young, L.W., and Jordan-Culler, T., "Hazards of Falling Debris to People, Aircraft, and Watercraft," Sandia Report SAND97-0805, Sandia National Laboratories, April 1997.
6. Coustenis, A., Hedman, N., and Kminek G., "COSPAR Policy on Planetary Protection," *Space Research Today* 211 (2021): 12–25.
7. European Space Agency (2023), *ESA Space Debris Mitigation Requirements*, ESSB-ST-U-007 Issue 1.
8. Furfaro, R., Reddy, V., Campbell, T., and Gray, B., "Tracking objects in cislunar space: the Chang'e 5 case," *AMOS Conf. Proc.* 2021.
9. Ganapathi, G.B., Birur, G.C., Tsuyuki, G.T., et al., "Active Heat Rejection System on Mars Exploration Rover—Design Changes from Mars Pathfinder," *Space Technology and Applications International Forum*, Albuquerque, NM, AIP Conf. Proc. 654.1 (2003): 206–217.
10. Gangestad, J.W., "Pack it in, Pack it out: Updating Policy and Standards for Cislunar Sustainability," The Aerospace Corporation, Center for Space Policy and Standards, 2023.
11. Gladman, B.J., "The Dynamical Evolution of Lunar Impact Ejecta," *Icarus*, 118 (1995): 302–321.
12. Gudkova, T.V., Lognonné, P.H., and Gagnepain-Beyneix, J., "Large impacts detected by the Apollo seismometers: Impactor mass and source cutoff frequency estimations," *Icarus*, 211.2 (2011): 1049–1065.
13. Heiken, G., Vaniman, D., and French, B., *Lunar Sourcebook: A User's Guide to the Moon*, Cambridge University Press, 1991.
14. Hermalyn, B. and Schultz, P.H., "Early-stage ejecta velocity distribution for vertical hypervelocity impacts into sand," *Icarus*, 209 (2010): 866–870.
15. Hermalyn, B., Schultz, P.H., Shirley, M., et al., "Scouring the surface: Ejecta dynamics and the LCROSS impact event," *Icarus*, 218 (2012): 654–665.
16. Holcomb, J.A., Mandel, R.D., and Wegmann, K.W., "The case for a lunar anthropocene," *Nature Geoscience*, 17 (2023): 2–4.
17. Housen, K. and Holsapple, K., "Ejecta from impact craters," *Icarus*, 211.1 (2011): 856–875.
18. Immer, C., Lane, J., Metzger, P., and Clements, S., "Apollo video photogrammetry estimation of plume impingement effects," *Icarus*, 214 (2011): 46–52.
19. Johnson, K., "Fly Me to the Moon: Worldwide Cislunar and Lunar Missions," Center for Strategic & International Studies, 2022.
20. "KAGUYA (SELENE) Slam Crashed to the Moon," *Japan Aerospace Exploration Agency (JAXA)*, 11 June 2009, https://global.jaxa.jp/press/2009/06/20090611_kaguya_e.html. Press Release.
21. Korycansky, D.G., Plesko, C.S., Jutzi, M., et al., "Predictions for the LCROSS mission," *Meteoritics & Planetary Science*, 44.4 (2009): 603–620.
22. Melosh, H.J., *Impact Cratering: A Geologic Process*, Oxford University Press, New York, 1989.
23. Metzger, P.T. and Mantovani, J.G., "The Damage to Lunar Orbiting Spacecraft Caused by the Ejecta of Lunar Landers," *Proceedings of the 17th Biennial International Conference on Engineering, Science, Construction, and Operations in Challenging Environments (Earth and Space 2021)*, 2021: 136–145.
24. Morse, D. (2021), *Intuitive Machines-1 Orbital Debris Assessment Report*, Intuitive Machines LLC, Houston, TX, version 1.1.
25. National Aeronautics & Space Administration (2011), *NASA's Recommendations to Space-Faring Entities: How to Protect and Preserve the Historic and Scientific Value of U.S. Government Lunar Artifacts*, NASA Human Exploration & Operations Directorate, Strategic Analysis & Integration Division.

26. National Aeronautics & Space Administration (2021), *Process for Limiting Orbital Debris*, Standard 8719.14C.
27. National Aeronautics & Space Administration (2022), *Implementing Planetary Protection Requirements for Space Flight*, Standard 8719.27.
28. Pokorny, P., Janches, D., Sarantos, M., et al., “Meteoroids at the Moon: Orbital Properties, Surface Vaporization, and Impact Ejecta Production,” *Journal of Geophysical Research: Planets*, 124 (2019): 752–778.
29. Schultz, P.H., Hermalyn, B., Colaprete, A., et al., “The LCROSS Cratering Experiment,” *Science*, 330 (2010): 468–472.
30. Shuvalov, V.V. and Trubetskaya, I.A., “Numerical Simulation of the LCROSS Impact Experiment,” *Solar System Research*, 42.1 (2008): 1–7.
31. United States Air Force (2021), *The US Air Force Mishap Prevention Program*, Air Force Instruction 91-202.
32. Singer, K., Jolliff, B.L., and McKinnon, W.B., “Lunar Secondary Craters and Estimated Ejecta Block Sizes Reveal a Scale-Dependent Fragmentation Trend,” *Journal of Geophysical Research: Planets*, 125.8 (2020): e2019JE006313.
33. Spremo, S., Turner, M., Caffrey, R.T., and Hine, B.P., “The Lunar Atmosphere and Dust Environment Explorer (LADEE) Mission,” *AIAA Space 2009 Conference and Exposition*, 2010, (No. ARC-E-DAA-TN1098).
34. United Nations (1967), *Treaty on principles governing the activities of States in the exploration and use of outer space, including the moon and other celestial bodies*.
35. United States Government (2019), *Orbital Debris Mitigation Standard Practices*.
36. Wei, M., Hu, C., Estevez, D., et al., “Design and flight results of the VHF/UHF communication system of Longjiang lunar microsatellites,” *Nature Communications*, 11.1 (2020): 3425.
37. Yamamoto, S., Kadono, T., Sugita, S., and Matsui, T., “Velocity distributions of high-velocity ejecta from regolith targets,” *Icarus*, 178 (2005): 264–273.
38. Yamamoto, S., Kadono, T., Sugita, S., and Matsui, T., “Cumulative Mass-Velocity Distribution of Impact Ejecta in Oblique Impacts,” *Lunar and Planetary Science XXXVII*, 2006.
39. Zeng, X., He, C., Oravec, H., et al., “Geotechnical Properties of JSC-1A Lunar Soil Simulant,” *Journal of Aerospace Engineering*, 23.2 (2010): 111–116.